The ground-state phase behavior of model Langmuir monolayers

S. B. Opps, B. G. Nickel, C. G. Gray, and D. E. Sullivan
Department of Physics and Guelph-Waterloo Physics Institute, University of Guelph, Guelph, Ontario, N1G 2W1 Canada

(Received 17 December 1999; accepted 7 April 2000)

A coarse-grained model for surfactant molecules adsorbed at a water surface is studied at zero temperature to elucidate ground-state tilt ordering. The surfactants are modeled as rigid rods composed of head and tail segments, where the tails consist of effective monomers representing methylene CH_2 groups. These rigid rods interact via site–site Lennard-Jones potentials with different interaction parameters for the tail–tail, head–tail, and head–head interactions. In this work, we study the effects due to variations in both the head diameter and bond length on transitions from untilted to tilted structures and from nearest-neighbor (NN) to next-nearest-neighbor (NNN) tilting. Coupling between tilt ordering and lattice distortion is also considered. We provide a molecular derivation of a scaling relation between tilt angles and distortion obtained previously by phenomenological arguments. Due to the discrete site–site nature of the model interactions, the predicted ground-state phase behavior is much richer than evidenced by models employing cylindrical rods. In particular, we have found transitions between different phases (i.e., NN–NN′ and NNN–NNN′) of similar symmetry, which may have experimental support. We have also examined the sensitivity of the transitions to details of the model, such as replacing Lennard-Jones head–head and head–tail potentials by purely repulsive interactions. © *2000 American Institute of Physics*. [S0021-9606(00)70525-3]

I. INTRODUCTION

In recent years, there has been considerable interest in the properties of monolayer systems such as self-assembled and Langmuir monolayers and Langmuir–Blodgett films.[1–11] In Langmuir monolayers, surfactants (i.e., amphiphilic organic molecules) are adsorbed at the air–water interface with the hydrophilic head groups in contact with the aqueous subphase while the hydrophobic hydrocarbon tails point away from the water. Although these monolayers appear structurally simple, they have quite complex phase behavior, displaying crystalline, hexatic, liquid, and gas phases. As such, they are comparable to other complex liquid systems such as smectic liquid crystals and phospholipid membranes. Despite differences in chemical detail, different Langmuir monolayers composed of fatty acids, alcohols, esters, or acetates share a similar ''generic'' phase diagram.[1–3] In the ''liquid-condensed'' region, this is characterized by at least three distinct phases (the so-called S, LS, and CS phases) in which the surfactant hydrocarbon chains are untilted on average and, at lower pressures, by at least four phases in which the chains are tilted toward either nearest neighbors (denoted L_2 and L_2'') or toward next-nearest neighbors (denoted L_2' and Ov). Since this phase diagram is applicable to a number of chemically different Langmuir monolayers, it is evident that general characteristics of the surfactant–water system must be responsible for the existence of the various tilt-ordered phases.

Despite the generic phase behavior of Langmuir monolayers, recent experimental work has shown that there *can be* fundamental differences in tilt ordering in the condensed phases due to the chemical structure of the surfactants. Teer *et al.*[5] and Shih *et al.*[7] have found that, whereas certain *n*-alkyl acetates and acids share similar phase diagrams, both having three tilted phases, L_2, L_2', L_2'', the corresponding alcohols and esters lack the L_2 phase. The authors attribute these variations to differences in head size and head–substrate interactions. Further investigation into the effects of structural detail is required to explain these differences. Schmid and Lange[12] addressed this problem from a phenomenological free-energy approach. Recently, Stadler *et al.*[13] and Stadler and Schmid[14] have performed Monte Carlo simulations in the constant molecular number, spreading pressure and temperature (NPT) ensemble and examined the phase diagram for two different values of the head/tail diameter ratio.

In the present work, we have done extensive ground-state calculations to elucidate the zero-temperature phase behavior of Langmuir monolayers. We use a rigid beaded-rod model for the surfactants similar to that employed in other recent ground-state studies,[15,16] but explicitly allowing for different diameters of the hydrophilic head and hydrophobic tail beads. Here, we study the effects of variations in the head-to-tail diameter ratio and intramolecular bond length on both transitions from untilted to tilted phases and transitions from nearest-neighbor (NN) to next-nearest-neighbor (NNN) tilted phases. By invoking symmetry arguments, we have derived a Landau free-energy expansion for the continuous untilted to tilted transition, whose coefficients are calculated *exactly*. By also calculating the energy exactly away from the untilted/tilted phase boundary, we have studied azimuthal tilt-ordering transitions between the NN and NNN phases. The analysis includes the effects of lattice distortions, and provides a molecular derivation of a scaling relation between

tilt angles and distortion which was previously derived by phenomenological arguments.[17] This scaling holds for both types of tilt ordering, since tilting in any azimuthal direction is accompanied by a corresponding distortion of the lattice.

Our calculations show that, at a fixed area per molecule, increasing either the bond length or the head/tail diameter ratio produces transitions from untilted to tilted phases. Tilt-ordering transitions from NNN to NN are also found to occur with increasing head/tail diameter ratio or *decreasing* bond length. For sufficiently small diameter ratio, the NNN–NN phase boundary moves to zero pressure. These effects of the head size on tilting transitions are in agreement with experiment[5,7] and with previous calculations[12] based on modeling the surfactant chains as cylindrical rods. Nonetheless, it is important to confirm these predictions using the more realistic site–site model, since the effects of head-size variations in this model have not been systematically studied in previous work.[15,16] Furthermore, earlier ground-state studies based on either cylindrical[18] or beaded[16,19] rods did not find evidence of the ''swiveling'' transition NNN–NN at low pressure. We present analytical calculations based on a simplified model (restricted to purely nearest-neighbor site–site interactions) which refines one used in Ref. 16 and which clearly elucidates the roles of both bond length and diameter mismatch on tilting.

In addition, the present beaded model produces other types of transitions, particularly ones between phases with the same type of azimuthal tilt ordering. Specifically, NN–NN′ and NNN–NNN′ transitions have been found within the NN–NNN coexistence domain. Although these transitions are metastable when the head–head and head–tail interactions are modeled as being purely repulsive (Rep model), the NN–NN′ phase boundary becomes briefly stable when those interactions are governed by a full Lennard-Jones potential (LJ model). Furthermore, the shape of the NN–NNN coexistence region differs substantially between the two models. There is evidence from recent experimental work[20] of similar transitions between phases of the same tilt-azimuth ordering, albeit between different NNN tilted phases, and it would be of interest to carry out further experimental studies to explore their occurrence.[21] In summary, we have completed a more extensive study than in previous work of the effects on ground-state tilt ordering due to head/tail diameter mismatch, bond length, and variations in the attractive nature of the head–group interactions.

The paper is organized as follows. In Sec. II we give an outline of the model and explanation for the choice of potentials. In Sec. III we discuss the details of the ground-state calculations. The results of these calculations are presented in Sec. IV and conclusions are drawn in Sec. V.

II. MODEL

The initial step to model the Langmuir monolayer is to simplify the structural features of the surfactants. The first level of approximation is to use the ''united atom'' scheme, whereby each methylene CH_2 group is represented by one monomer unit. A further reduction of complexity is afforded by coarse-graining the hydrocarbon backbone such that a series of CH_2 groups, from 3 to 5, is combined into one effective monomer and the effective monomers are linked by rigid bonds (Fig. 1).[16] The head group is represented by a single effective monomer, while each tail contains n_t effective monomers. Adjacent pairs of monomers (both tail–tail and head–tail) are separated by a bond length denoted σ_l. Although this rigid-rod model would appear to be a drastic simplification, similar models have been considered in previous studies[15,16,19,22] and we examine it here in order to focus on the effects of bond length and head/tail diameter mismatch on tilting transitions.

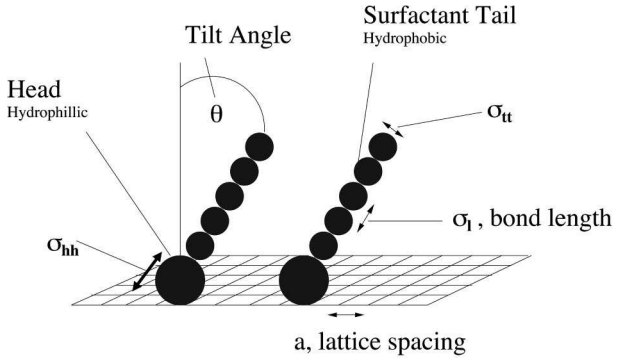

FIG. 1. A coarse-grained model of a surfactant chain on water. The surfactants are treated as rigid rods with a characteristic bond length σ_l, head diameter σ_{hh}, tail diameter σ_{tt}, and tail length which depends on the number of effective monomers in the chain. The surfactant heads are grafted onto a planar lattice with lattice spacing a.

Due to their chemical composition, the surfactants are arranged so that their (hydrophilic) heads are held in contact with the water substrate while the (hydrophobic) tails are free to point away. However, in the present model, explicit details of the surfactant–water interactions are not accounted for and the water is treated as a solid surface. At low temperature, there should not be significant diffusion of the head groups across the water surface and, therefore, this approximation should not drastically alter the characteristics of the phase diagram.

The interactions between tail beads on different molecules are modeled by a Lennard-Jones site–site potential,

$$V_{tt}^{\mathrm{LJ}}(r)=4\varepsilon_{tt}\left(\left(\frac{\sigma_{tt}}{r}\right)^{12}-\left(\frac{\sigma_{tt}}{r}\right)^{6}\right). \tag{1}$$

Elsewhere, using Monte Carlo simulations we have investigated the nonzero temperature behavior of these model systems.[23] For the purpose of computational efficiency, the head–head and head–tail interactions between different molecules were modeled as being repulsive with the following *truncated and shifted* Lennard-Jones potential:

$$V_{\alpha\beta}^{ts}(r)=\begin{cases} V_{\alpha\beta}^{\mathrm{LJ}}(r)-V_{\alpha\beta}^{\mathrm{LJ}}(r_{\alpha\beta}^{\min}), & r\leqslant r_{\alpha\beta}^{\min} \\ 0, & r>r_{\alpha\beta}^{\min}, \end{cases} \tag{2}$$

with mixing rules

$$\varepsilon_{\alpha\beta}=(\varepsilon_{\alpha\alpha}\varepsilon_{\beta\beta})^{1/2}, \quad \sigma_{\alpha\beta}=(\sigma_{\alpha\alpha}+\sigma_{\beta\beta})/2, \tag{3}$$

where $\varepsilon_{\alpha\beta}$ measures the strength of the interaction, $\sigma_{\alpha\beta}$ gives the range of the potential, α,β are indices labeling which types of sites (i.e., head and/or tail) are interacting, and $r_{\alpha\beta}^{\min}=2^{1/6}\sigma_{\alpha\beta}$. In the following, we take $\varepsilon_{tt}=\varepsilon_{hh}$. How-

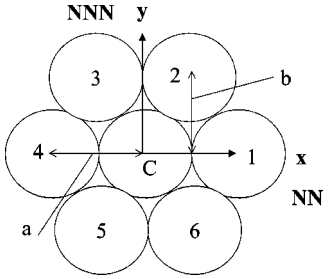

FIG. 2. Nearest- and next-nearest neighbor tilting directions. Nearest-neighbor tilting is in the x direction and next-nearest-neighbor tilting is in the y direction.

ever, although the potential (2) is well suited for the simulations, it leads to inherent numerical problems for the ground-state analysis, since its higher-order derivatives contain discontinuities. To compensate for this drawback, and to ensure consistency between the simulations and the ground-state analysis, the truncated and shifted potential (2) was numerically fit with a smooth function

$$V_{\alpha\beta}^{\mathrm{fit}}(r)=f\varepsilon_{\alpha\beta}\exp(gx_{\alpha\beta}^2\ln x_{\alpha\beta}+h\ln x_{\alpha\beta}/x_{\alpha\beta}), \tag{4}$$

where

$$f=\exp(-0.017\,536\,1),\quad g=-8.861\,792,$$
$$h=-3.181\,784,\quad x_{\alpha\beta}=\left(\frac{r}{\sigma_{\alpha\beta}}\right)^2, \tag{5}$$

which was used as a replacement for (2).

Although we indicated that the head–head and head–tail interactions are treated as being purely repulsive, we have also considered, for comparative purposes, the model where all interactions are the same and governed by the full Lennard-Jones potential (1). For economy, we shall from now on refer to the latter as the **LJ model**. The model where tail–tail interactions are governed by the Lennard-Jones potential, but where head–head and head–tail interactions are determined by $V_{\alpha\beta}^{\mathrm{fit}}$, will be refered to as the **Rep model** (short for repulsive).

III. GROUND-STATE CALCULATIONS

A. Landau expansion

In this work, we will analyze the ground-state behavior of the model in order to gain some insight into the tilting order at low temperatures, which should also be relevant to properties at elevated temperatures. From experimental[1–3,5–8] and theoretical results,[12,15,17,18] one expects to find an untilted phase and at least two tilt-ordered structures with tilting in either the NN or NNN azimuthal directions (see Fig. 2). By fixing the heads of the molecules onto a lattice, we will monitor both changes in the tilt structure and the lattice geometry as the area per molecule is varied. In the untilted state, the lattice has hexagonal symmetry, whereas, upon tilting, the lattice undergoes orthorhombic distortions to a centered rectangular structure. To accommodate for these distortions, the lattice parameters a' and b' of the distorted lattice (see Fig. 2) are expressed as follows:

$$a'^2=\frac{2}{\sqrt{3}}Ae^{\alpha}=a^2e^{\alpha},\quad b'^2=\frac{\sqrt{3}}{2}Ae^{-\alpha}=b^2e^{-\alpha}, \tag{6}$$

where α is the distortion parameter and the area per molecule, $A=a'b'=ab$, is preserved upon distortion. Note that for the undistorted hexagonal lattice ($\alpha=0$), we recover the standard relations $b'=b=\sqrt{3}/2\,a$, $a'=a$, and $A=\sqrt{3}/2\,a^2$.

Anticipating that the tilted/untilted transition is second order in nature, one can perform a Landau expansion of the free energy per molecule in the distortion, α, and tilt, $\sin(\theta)$, order parameters. At zero temperature, the free energy is equal to the ground-state energy E. *A priori*, we do not know the minimal orders to which the expansion must be calculated in order to distinguish between tilting in the NN and NNN directions. As shown in the Appendix as well as from arguments below, the minimal orders turn out to be sixth order in $\sin(\theta)$ and third order in α. Hence, the Landau expansion of the ground-state energy is

$$\begin{aligned}E=&E_0+E_{2\theta}\sin^2(\theta)+E_{4\theta}\sin^4(\theta)+E_{6\theta}\sin^6(\theta)\\&+E_{2\theta,\alpha}\sin^2(\theta)\alpha+E_{4\theta,\alpha}\sin^4(\theta)\alpha+E_{2\alpha}\alpha^2\\&+E_{2\theta,2\alpha}\sin^2(\theta)\alpha^2+E_{3\alpha}\alpha^3+\cdots,\end{aligned} \tag{7}$$

where the various coefficients are expressed in terms of the intermolecular site–site potentials in the Appendix. The absence of odd-order terms in $\sin(\theta)$ is demonstrated in the Appendix. There, it is also shown that differences between tilting in the NN and NNN directions only occur in the coefficients $E_{6\theta}$,$E_{2\theta,\alpha}$,$E_{2\theta,2\alpha}$, and $E_{4\theta,\alpha}$.

The expression (7) is similar in form to the phenomenological free energy derived purely from symmetry considerations by Kaganer and Indenbom,[17] as given by their equation (6) (see also Refs. 3 and 8). Note that in Ref. 17, the molecules are not treated as linear rods, but as kinked rods in an all-*trans* configuration. As such, the molecular backbone planes can exhibit herringbone ordering which also causes distortions of the lattice. This sort of distortion is different from the type which occurs solely due to tilting, studied in this work. Note that the free energy of Ref. 17 contains undetermined coefficients which are dependent on temperature, whereas we calculate the free energy exactly at zero temperature.

In order to assess which of the phases, i.e., untilted or tilted in NN or NNN directions, is most stable, one needs to minimize the energy in (7). First minimizing with respect to α gives, to $\mathcal{O}(\sin^4(\theta))$,

$$\begin{aligned}\alpha_{\min}=&-\frac{E_{2\theta,\alpha}}{2E_{2\alpha}}\sin^2(\theta)\\&-\left(E_{4\theta,\alpha}-\frac{E_{2\theta,2\alpha}E_{2\theta,\alpha}}{E_{2\alpha}}+\frac{3E_{3\alpha}E_{2\theta,\alpha}^2}{4E_{2\alpha}^2}\right)\frac{\sin^4(\theta)}{2E_{2\alpha}}.\end{aligned} \tag{8}$$

One observes that, to first order, $\alpha_{\min}\propto\sin^2(\theta)$, as first predicted in Ref. 17. As described in the Appendix, the coefficient $E_{2\theta,\alpha}$ has the same magnitude but opposite sign for tilting toward NN and NNN directions. This is physically consistent with experimental[3,6–8] and theoretical[12,18,19] findings that the lattice expands in the direction of tilt. Referring

to the definitions of the distorted lattice constants a' and b' in (6), this implies that α should be positive (negative) for tilt toward NN (NNN) directions, which is reflected by the differing signs of the coefficient $E_{2\theta,\alpha}$.

With $\alpha_{\min}$ given by (8), the energy becomes

$$E_{\min,\alpha}=B\sin^2(\theta)+C\sin^4(\theta)+D\sin^6(\theta)+\cdots, \tag{9}$$

where

$$B\equiv E_{2\theta},$$

and where the renormalized coefficients are

$$C=E_{4\theta}-\frac{E_{2\theta,\alpha}^2}{4E_{2\alpha}},$$
$$D=E_{6\theta}-\frac{E_{4\theta,\alpha}E_{2\theta,\alpha}}{2E_{2\alpha}}+\frac{E_{2\theta,2\alpha}E_{2\theta,\alpha}^2}{4E_{2\alpha}^2}-E_{3\alpha}\left(\frac{E_{2\theta,\alpha}}{2E_{2\alpha}}\right)^3. \tag{10}$$

According to Landau theory, provided $C>0$, (9) predicts a second-order transition from an untilted to a tilted phase at

$$B=0\,. \tag{11}$$

This equation can be solved numerically for the critical area A_c at the transition using a Newton–Raphson procedure. The parameter B is given explicitly in the Appendix [see (A6), (A7), and (A17)] in terms of the site–site intermolecular potential energy on an undistorted hexagonal lattice. The lattice sums required to evaluate B were carried out numerically over 20 neighboring shells. Note that for $B>0$, the minimum in the free energy is achieved at $\sin(\theta)=0$. To determine which of the tilted phases is more stable, we must evaluate (9) along the phase boundary where $B=0$. As shown by (10), C is found to be the same for both NN and NNN phases. It is only at sixth order in $\sin(\theta)$ that differences occur. Hence, along the critical tilted/untilted phase boundary, the stable tilt direction (NN or NNN) is that which has the lower value of the Landau coefficient D, in agreement with arguments of Ref. 17. This coefficient was also evaluated numerically by performing the lattice sums given in the Appendix.

As a final note, we find that the continuous nature of the tilted/untilted transition is destroyed and becomes weakly first order when $V_{\alpha\beta}^{ts}(r)$ is used instead of $V_{\alpha\beta}^{\text{fit}}(r)$. This is a consequence of the discontinuous nature of the site–site potential $V_{\alpha\beta}^{ts}$, which invalidates the Landau expansion by producing discontinuities in second-order and higher-order derivatives of the site–site potential. The resulting first-order transitions slightly shift all the phase boundaries reported here.

B. A simplified model

Before proceeding to examine phase diagrams generated from our exact ground-state analysis, we shall derive a model to describe the tilting transition based on a simplified physical argument. Although this approach is an approximation and is not capable of elucidating which of the NN or NNN phases is more stable, it nevertheless provides some important physical insight. Consider the following picture. First, we assume that only interactions between *adjacent* monomers on nearest-neighbor molecules are relevant. Since the separation between parallel monomers on different rods (i.e., monomers lying in the same horizontal plane) is preserved upon tilting at fixed lattice spacing a, the only relevant lengths that play a role in tilting are d_o, d, and d', defined in Fig. 3. For simplicity, this picture is drawn assuming tilt of molecules toward their nearest neighbors. The untilted structure, Fig. 3(a), corresponds to $d_o=d=d'$, whereas the tilted state, Fig. 3(b), requires that $d<d_o<d'$. If the lattice spacing a is small enough, then $d_o\sim r_{\text{tt}}^{\min}=2^{1/6}\sigma_{tt}$. In this case, the energies associated with both separations d and d' are greater than those corresponding to the distance d_o and the vertical state will be favored. For larger lattice spacing, it is conceivable that, compared to the untilted distance d_o, monomers separated by d will reach a lower energy, whereas those separated by d' will reach higher energies. If the loss in energy for monomers separated by d is greater than the energy gain for those separated by d', the tilted state is more stable.

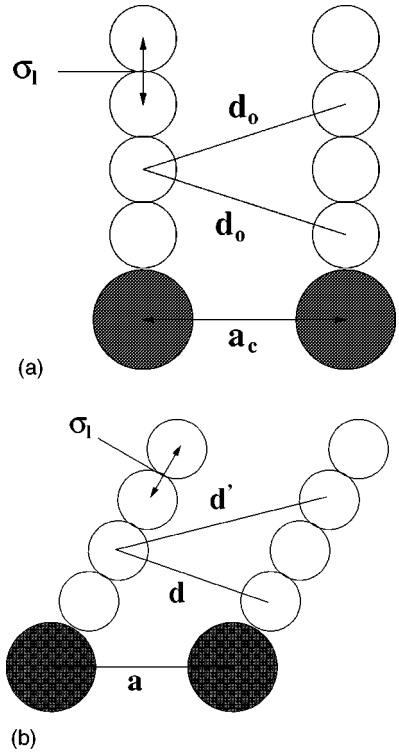

FIG. 3. Optimal distances for tilting transitions. For the untilted structure, the optimal separation is denoted d_o (a). To drive a tilting transition (b), it is required that the loss in energy for monomers separated by d is greater than the energy gain for those separated by d'.

To determine the critical lattice spacing a_c where the tilt transition occurs, one needs to explicitly calculate the interaction energy of a central molecule C with its six nearest neighbors. Again, for purposes of finding this phase boundary, the energies for NN and NNN tilting are equivalent. Choosing the NNN tilt direction, upon tilting, molecules 1 and 4 have the same interactions with the central molecule C (refer to Fig. 2) as when they are untilted. Therefore, we only need to consider interactions of C with molecules 2,3,5, and 6. The distance d is then equal to the distance from site 2 to a site one bond length (σ_l) along molecule C, while d' is

equal to the distance from site C to a site one bond length along molecule 2. These are straightfowardly found to be given by

$$d^2 = a^2 + \sigma_l^2 - \sqrt{3}\, a\, \sigma_l \sin(\theta),$$
$$d'^2 = a^2 + \sigma_l^2 + \sqrt{3}\, a\, \sigma_l \sin(\theta). \tag{12}$$

With the distances d and d' calculated, the total interaction potential energy of molecule C with its neighbors *relevant* to tilting is

$$V_C = 4(V_{ht}(d) + V_{ht}(d') + (n_t - 1)[V_{tt}(d) + V_{tt}(d')]), \tag{13}$$

where $V_{\alpha\beta}(r)$ is the monomer–monomer potential between monomers of type α and β (with h=''head,'' t=''tail''), and n_t is the number of tail monomers on a molecule.

At the tilting transition, where $a = a_c$,

$$\left(\frac{d^2 V_C(\theta)}{d\theta^2}\right)_{\theta=0, a=a_c} = 0. \tag{14}$$

Using (12) and (13), and given the condition that at $\theta = 0, d_o = d = d'$, one can solve (14) to obtain a relation for the transition value of d_o

$$V''_{ht}(d_o) + (n_t - 1) V''_{tt}(d_o) = \frac{1}{d_o}[V'_{ht}(d_o) + (n_t - 1) V'_{tt}(d_o)], \tag{15}$$

where

$$V'_{\alpha\beta}(r) = \frac{dV_{\alpha\beta}(r)}{dr}$$

and

$$V''_{\alpha\beta}(r) = \frac{d^2 V_{\alpha\beta}(r)}{dr^2}.$$

We shall refer to the approximate method (15) for determining the transition between tilted and untilted states as the **Approx method** in contrast to the **Landau method** based on Eq. (11).

C. NN–NNN coexistence

At areas per molecule greater than A_c, one expects to find tilting transitions from NN to NNN azimuthal ordering which, for small distortions of the lattice, should be first order, since the two phases have different symmetries. To determine this phase transition, we first minimize the unexpanded energy per molecule given by (A1) with respect to tilt-angle θ and the distortion parameter α at fixed area A, using a two-dimensional Newton–Raphson procedure. By repeating this calculation at different areas to obtain $E_{\min}^{\mathrm{NN}}(A)$ and $E_{\min}^{\mathrm{NNN}}(A)$, the coexisting areas are then determined from a common-tangent construction.

To examine how different physical features of surfactants affect tilting transitions, we varied a number of adjustable parameters in our model and computed the resulting phase diagrams. In particular, we have focused on the effects that varying bond length and head diameter have on the ground-state phase behavior. These findings are described in the following section.

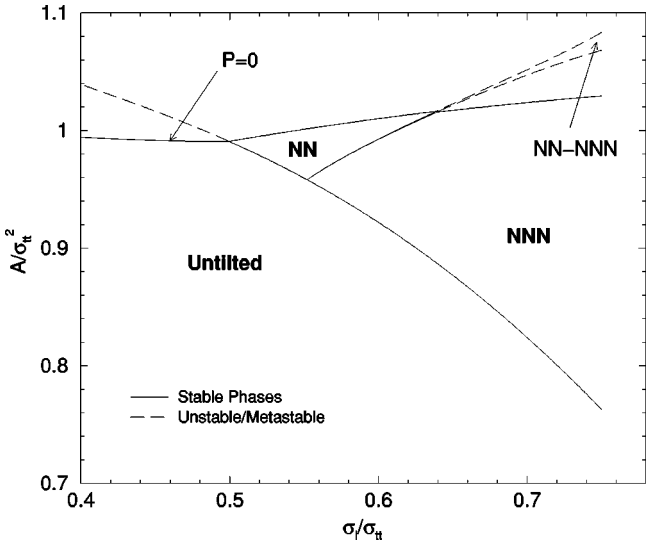

FIG. 4. Ground-state phase diagram resulting from variations in bond length σ_l, in the Rep model, with $\sigma_{tt} = \sigma_{hh}$ and $n_t = 4$.

IV. RESULTS

A. Dependence on bond length

1. Tilted/untilted phase boundary

Using (11) with the Rep model, with $n_t = 4$ and $\sigma_{tt} = \sigma_{hh}$, we varied the bond length σ_l and calculated the tilted/untilted phase boundary, shown in Fig. 4. The qualitative shape of this boundary can be understood with the Approx method, using the fact that at $\theta = 0$, $d_o = d = d'$,

$$a_c^2 + \sigma_l^2 = d_o^2, \tag{16}$$

[as shown in Fig. 3(a)] and the fact that $A_c = \sqrt{3}/2\, a_c^2$. Hence,

$$A_c = \frac{\sqrt{3}}{2}[(d_o^2 - \sigma_l^2)], \tag{17}$$

describing a parabola in the (A, σ_l) plane. For the case where $\sigma_{tt} = \sigma_{hh}$ and all interactions are governed by the LJ model, (15) becomes (*independent* of n_t)

$$V''_{tt}(d_o^{\mathrm{LJ}}) = \frac{1}{d_o^{\mathrm{LJ}}} V'_{tt}(d_o^{\mathrm{LJ}}), \tag{18}$$

which yields

$$d_o^{\mathrm{LJ}} = (\tfrac{7}{2})^{1/6} \sigma_{tt}. \tag{19}$$

According to (19), it is clear that $d_o^{\mathrm{LJ}} > r_{tt}^{\min} = 2^{1/6}\sigma_{tt}$. Using the Rep model, (15) must be solved numerically. In this case (again with $\sigma_{hh} = \sigma_{tt}$ and $n_t = 4$), we find that $d_o^{\mathrm{Rep}} = 1.232\,751\sigma_{tt}$, which differs very little from (19).

The relations (16)–(19) based on the Approx method do not reproduce the exact results determined from (11), but overestimate the critical area A_c for a given bond length σ_l by about 10%. Nonetheless, these relations predict the same

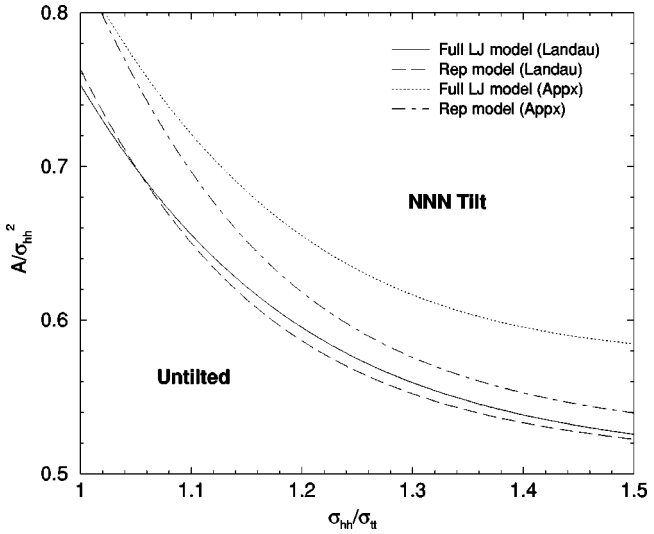

FIG. 5. Comparison of the tilted/untilted phase boundaries using the Rep-(Landau), LJ(Landau), Rep(Approx), and LJ(Approx) models, for fixed bond length $\sigma_l = 0.75\,\sigma_{tt}$, $n_t = 4$, and varying head diameter σ_{hh}.

qualitative features as those displayed in Fig. 4, in particular the feature that, for fixed area A, increasing σ_l stabilizes the tilted phase.[24]

2. NN–NNN transition

As mentioned earlier, we are only able to detect differences between NN and NNN energies at sixth order in $\sin(\theta)$. Utilizing (10) with the Rep model for $\sigma_{hh} = \sigma_{tt}$ and $n_t = 4$, it is found that the NN–NNN transition occurs at a bond length of $\sigma_{lc}^{\mathrm{NN-NNN}} = 0.551\,959\,\sigma_{tt}$ and an area of $A_c^{\mathrm{NN-NNN}} = 0.957\,975\,\sigma_{tt}^2$, which corresponds to a lattice spacing of $a_c^{\mathrm{NN-NNN}} = 1.051\,748\,3\,\sigma_{tt}$. This NN–NNN transition which occurs at a point along the second-order tilted/untilted boundary must coincide with the termination of the NN–NNN first-order line. To determine this first-order line, we followed the method described in Sec. III C to obtain the results displayed in Fig. 4. Referring to the stable portions of the phase diagram ($P > 0$, where $P = -dE/dA$ is the spreading pressure), one observes that, for fixed area (with $A > A_c^{\mathrm{NN-NNN}}$), increasing σ_l tends to stabilize the NNN phase. Alternatively, for fixed bond length, it is clear that increasing the area drives the system from NNN towards NN tilting.

B. Dependence on tail/head diameter mismatch

1. Tilted/untilted phase boundary

Having studied the phase diagram for fixed head diameter while varying the bond length, we now investigate the tilt ordering which results from fixing the bond length at $\sigma_l = 0.75\,\sigma_{tt}$ and varying the head diameter for both LJ and Rep models. The results are shown in Figs. 5–7. To determine the tilted/untilted boundary, (11) was again employed. However, by evaluating the coefficient D in (10) one finds that, in contrast to the previous results for varying bond length, the NNN tilted structure remains the stable phase along the entire second-order boundary (Fig. 5).

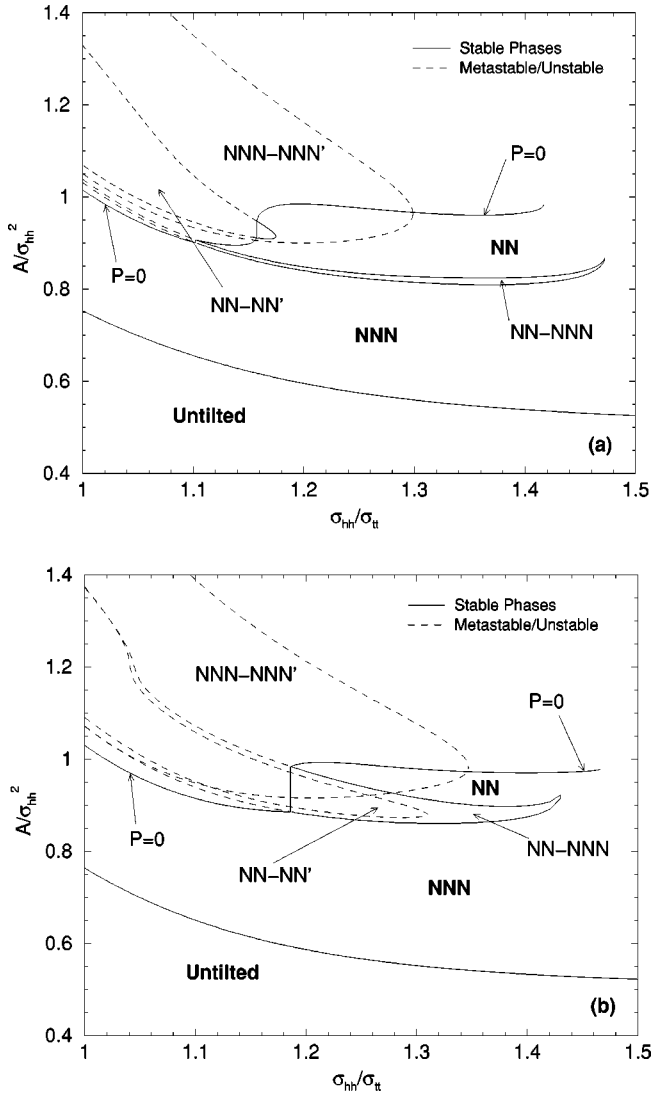

FIG. 6. Ground-state phase diagrams resulting from variations in the head diameter, for fixed bond length $\sigma_l = 0.75\,\sigma_{tt}$ and $n_t = 4$. Note that both LJ (a) and Rep (b) models exhibit NN–NNN′, NN–NN′, and NNN–NNN′ transitions. However, the NN–NN′ and NNN–NNN′ coexisting phases are either unstable or metastable, as indicated by the dashed lines, except for a portion of the NN–NN′ transition in (a). Note also that the NN–NNN coexistence curves differ dramatically between the two models.

The power-law behavior of the tilted/untilted phase boundary in Figs. 5 and 6 can again be understood using the Approx method. By explicitly solving for d_o in (15), for the LJ model, we find [generalizing (19)]

$$\left(\frac{d_o^{\mathrm{LJ}}}{\sigma_{tt}}\right)^6 = \frac{7}{2}\,\frac{[(n_t-1)+(\sigma_{ht}/\sigma_{tt})^{12}]}{[(n_t-1)+(\sigma_{ht}/\sigma_{tt})^{6}]}, \tag{20}$$

which can be combined with the relationship (17). Setting $\sigma_l = 0.75\,\sigma_{tt}$ and $n_t = 4$, we examine the predictions of (20) for two particular values, $\sigma_{hh}/\sigma_{tt} = 1.2$ and 1.4 which, following from the mixing rule (3), give $\sigma_{ht}/\sigma_{tt} = 1.1$ and 1.2, respectively. The results are given in Table I. It is seen that d_o^{LJ} is *greater* than the minimum of the head–tail Lennard-Jones potential, at $r_{ht}^{\min} = 2^{1/6}\sigma_{ht}$, which has the values

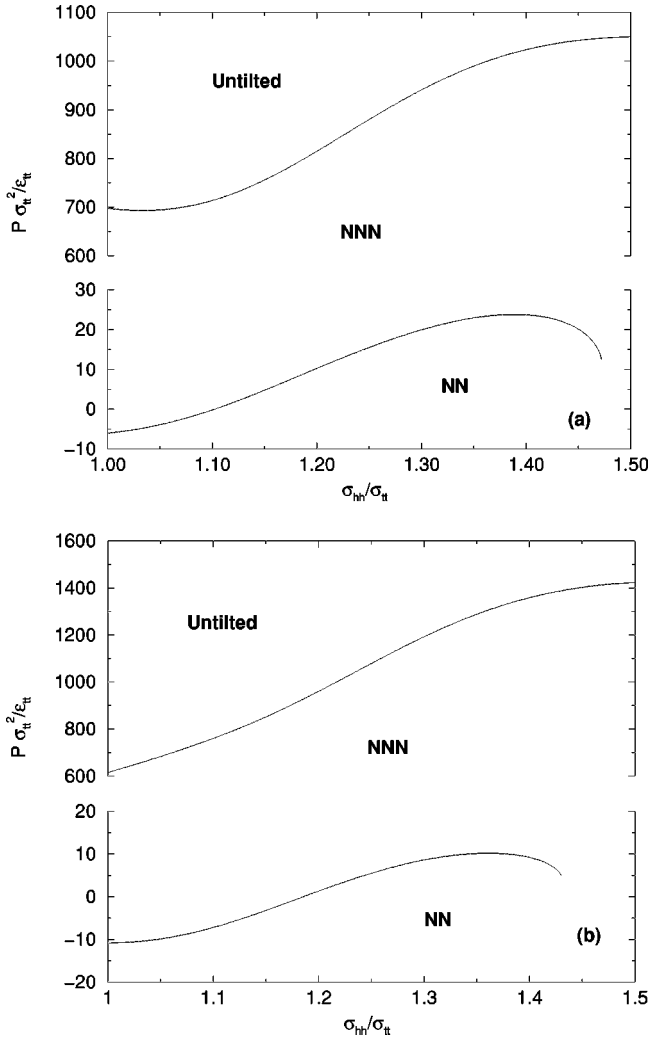

FIG. 7. The same ground-state phase diagrams as Figs. 6 but in the pressure/head-diameter plane, for both LJ (a) and Rep (b) models. Note that the two phase boundaries are plotted using different pressure scales.

$$\frac{r_{ht}^{\min}}{\sigma_{tt}} = 1.234\,708 \quad (\sigma_{hh}/\sigma_{tt}=1.2),$$
$$= 1.346\,954 \quad (\sigma_{hh}/\sigma_{tt}=1.4). \tag{21}$$

Using the Rep model, (15) must be solved numerically. This yields slightly different results, given in Table II. We see that $d_o^{\rm rep} < d_o^{\rm LJ}$ and correspondingly $A_c^{\rm rep} < A_c^{\rm LJ}$. With increasing σ_{hh}/σ_{tt}, $d_o^{\rm rep}$ approaches and actually becomes slightly less than $r_{ht}^{\min}$.

The approximate results for the tilted/untilted phase boundary are compared with the exact Landau results in Fig. 5. The same qualitative trends are exhibited, although the Approx method overestimates the critical area A_c at the transition for both the LJ and Rep models and also exaggerates the differences between the two models. These are due to the fact that the Approx method neglects attractive tail–tail interactions beyond those between nearest-neighbor monomers.

TABLE I. Results from the approximate calculation of the tilting transition for $\sigma_l = 0.75\,\sigma_{tt}$ and $n_t = 4$, using the LJ model.

	$\sigma_{hh}/\sigma_{tt}=1.2$	$\sigma_{hh}/\sigma_{tt}=1.4$
d_o/σ_{tt}	1.285 023	1.382 010
a_c/σ_{hh}	0.869 539 8	0.829 141
A_c/σ_{hh}^2	0.654 801	0.595 371

TABLE II. Results from the approximate calculation of the tilting transition for $\sigma_l = 0.75\,\sigma_{tt}$ and $n_t = 4$, using the Rep model.

	$\sigma_{hh}/\sigma_{tt}=1.2$	$\sigma_{hh}/\sigma_{tt}=1.4$
d_o/σ_{tt}	1.260 995	1.346 530
a_c/σ_{hh}	0.844 759	0.798 801
A_c/σ_{hh}^2	0.618 010	0.552 596

The main feature shown by Figs. 5 and 6 is that, for a fixed packing fraction A/σ_{hh}^2, increasing the head diameter σ_{hh} drives a transition from the untilted to the NNN tilted phase. The negative slope of the tilted/untilted phase boundaries in Figs. 5 and 6 is a simple consequence of the fact that increasing the head diameter increases the separation between untilted tails. In order to maintain an optimal tail separation d [see Fig. 3(b)] near the minimum of the tail–tail site–site potential, the tails must tilt towards their neighbors. This feature agrees with the findings of earlier studies[12,18] using cylindrical rods that tilting is favored by increasing the head/tail diameter mismatch.

The same phase boundaries as in Fig. 5 and 6 are shown in Fig. 7 in terms of pressure versus head diameter. Here, it is clearly seen that, for fixed pressure, increasing σ_{hh} drives a transition from untilted to the NNN tilted phase. Therefore, at larger σ_{hh}/σ_{tt}, a larger pressure is required to drive a transition from tilted to the untilted phase and the latter exists over a wider pressure range. Note that, in agreement with Ref. 15, we find that the NN phase exists only at very low pressure.

2. NN–NNN transition

Turning to the NN–NNN transition, we shall first consider the trends shown in Figs. 6 and 7 that are similar for both LJ and Rep models. At fixed area, increasing the head diameter drives a transition from the NNN to the NN tilted phase. As seen for both models in Fig. 7, the NN phase becomes unstable (i.e., only occurs at $P<0$) for sufficiently small σ_{hh}/σ_{tt}, as found by Schmid and Lange[12] using a model of cylindrical rods with variable-sized head groups.

The nature of the phase transition from NNN to NN with increasing head diameter is revealed by the behavior of both the tilt angle and distortion. As noted, for smaller head diameters the NNN tilted phase is favored. As the head diameter is increased at fixed spreading pressure, the area per molecule necessarily increases. In order to maintain the optimal separation between parallel strips of tilted tails, the lattice must expand in the direction of tilt and contract in the direction perpendicular to the tilt. In response to both the increase in area and the expansion in the tilt direction, the tilt angle must also increase in order to maintain the optimal tail separation between neighboring molecules. At a sufficiently large head diameter, the expansion of the lattice in the NNN direction becomes too large and, referring to Fig. 2, it is no longer possible to maintain an optimal packing of a central

molecule C within the ''pocket'' formed by its four neighbors 2, 3, 5, and 6. At this point, the tilt changes to the NN direction, with the dilation of the lattice now in the NN direction. Further increases of the head diameter result in additional increases in the magnitude of the tilt angle and distortion until, at $\sigma_{hh,c} \sim 1.42\,\sigma_{tt}$, there is a collapse of the NN–NNN coexistence curve as a critical point is asymptotically approached, at which the two phases attain the same centered rectangular structure (the tilt angles in both phases approach approximately 40° at this point). In this region, it appears that the repulsive nature of the head-head interactions dictates much of the phase behavior.

It is interesting to note that, due to their discrete site–site nature, both the LJ and Rep models display other phase transition phenomena. In particular, there is stable, metastable, and unstable coexistence between different NN phases (denoted NN–NN′) and, also between different NNN phases (denoted NNN–NNN′). For a given tilt direction (for example, NN), it is possible to have phase equilibrium between different NN phases which have different tilt angles ($\theta_{\mathrm{NN}}, \theta_{\mathrm{NN}'}$) and different distortion parameters ($\alpha_{\mathrm{NN}}, \alpha_{\mathrm{NN}'}$). However, it is only in a small region of parameter space that stable coexistence occurs. As seen in Fig. 6(a), there is a small portion of the NN–NN′ phase coexistence which is stable, residing within the generic NN phase at pressures $P > 0$. Stable NNN–NNN′ coexistence does not occur, since it is either unstable at $P < 0$ or lies within the region of NN stability and is therefore metastable. The phase equilibria patterns change substantially when using the Rep model, as shown in Fig. 6(b). Whereas, with the LJ model, the NN–NNN coexistence width is very narrow, the Rep model causes a broadening of this width. Another feature of Fig. 6(b) is that there is no stable NN–NN′ and NNN–NNN′ coexistence. Although a segment of the NN–NN′ coexistence is stable for the LJ model, it is located completely within the NN–NNN coexistence region for the Rep model and is, therefore, metastable.

V. CONCLUSIONS

It has been demonstrated that the ground-state phase behavior of the model Langmuir monolayer is sensitively dependent on both variations in the intramolecular bond length and the head diameter. By grouping several CH_2 groups into effective monomers and linking these monomers with rigid bonds, we have attempted to model the bead-like nature of the surfactant backbone chain as realistically as possible. The importance of the discrete site–site nature of the surfactant–surfactant interactions is displayed in the phase diagrams of Figs. 4–7. In Fig. 4, for fixed area, one observes that increasing the bond length drives the system from an untilted to a tilted phase. Furthermore, at an area ($A > A_c^{\mathrm{NN-NNN}}$) beginning in the NN tilted phase, increasing the bond length leads to a swiveling transition into the NNN phase. It is apparent that variations in the bond length play a fundamental role in determining the tilt ordering at zero temperature, which has received relatively little previous study.[15,16] It is surmised that this will also be true at nonzero temperature, which will be examined elsewhere.[23]

The main focus of this study was to analyze the dependence of the head/tail diameter mismatch on the phase behavior of model Langmuir monolayers. In the more condensed regime (i.e., smaller areas), we find that increasing the head diameter leads to a stabilization of the tilted phase; see Fig. 5. At the more dilute end of the scale, beginning in the NNN phase, increasing the head diameter at fixed area drives the system from the NNN to the NN tilted phase. We have also seen that the coexistence curves differ significantly between the Rep and LJ models. Whereas with the LJ model the NN–NN′ coexistence is stable in a small range of σ_{hh}/σ_{tt}, it becomes metastable with the Rep model (the NNN–NNN′ phase coexistence only exists within the metastable and unstable portions of the phase diagrams for both models). As mentioned in the Introduction, recent experiments[20] have found evidence of similar first-order transitions between phases of the same azimuthal tilt-ordering symmetry, and further studies[21] might provide additional insight to the details of these phase transitions. In addition to differences between the Rep and LJ models for the NN–NN′ and NNN–NNN′ transitions, the structure of the NN-NNN coexistence region differs appreciably between the models. Thus, it is clear that variations in the head diameter determine the overall tilt ordering of the system and the finer details of the coexistence curves depend on the precise nature (e.g., LJ or Rep) of the site–site potentials.

ACKNOWLEDGMENT

This work is supported by a grant from the Natural Sciences and Engineering Research Council (Canada).

APPENDIX: DETAILS OF THE FREE ENERGY EXPANSION

At zero temperature, the free energy is equal to E, the total potential energy per molecule, and thus the expansion coefficients in (7) are just derivatives of the potential energy. Let us examine these coefficients to determine which ones vanish. Additionally, as discussed in Sec. III A, we need to find the minimum number of terms required in the energy expansion in order to be able to differentiate between NN and NNN phases.

Since we are considering a system with uniform tilt (either in the NN or NNN direction) and no sublattice ordering, all molecules are equivalent. The energy per molecule is explicitly given by the sum over all of the j neighbors surrounding any molecule i of the molecule–molecular pair interaction,

$$E = \sum_{j \neq i} \sum_{\gamma,\delta} V_{\gamma\delta}(r_{\gamma\delta}^{ij}) \equiv \sum_{j \neq i} \sum_{\gamma,\delta} U_{\gamma\delta}((r_{\gamma\delta}^{ij})^2), \tag{A1}$$

where $r_{\gamma\delta}^{ij}$ is the distance from site γ on molecule i to site δ on molecule j, and $V_{\gamma\delta}(r)$ is the site–site potential between sites γ and δ. Since in practice this is a function of r^2 [see (1) and (4), (5)], it is convenient to express $V_{\gamma\delta}(r) = U_{\gamma\delta}(r^2)$. For two molecules tilted in the same direction and separated by lattice vector $\mathbf{r_{ij}}$, the distance between two nonparallel sites is

$$(r_{\gamma\delta}^{ij})^2 = r_{ij}^2 + z_{\gamma\delta}^2 \pm 2\, z_{\gamma\delta}\, \mathbf{r_{ij}} \cdot \hat{\mathbf{n}} \equiv (\mathbf{r}_{\gamma\delta}^{(\pm)})^2,$$

where

$$\hat{\mathbf{n}} = \cos(\theta)\hat{\mathbf{k}} + \sin(\theta)\hat{\mathbf{l}}$$

is the unit vector in the direction of molecular axes, $\hat{\mathbf{k}}$ is the unit vector normal to the monolayer plane, and $\hat{\mathbf{l}}$ is a unit vector in the monolayer plane. The distance $z_{\gamma\delta}$ is the separation between sites γ and δ along the molecule chain given in integral numbers of the bond length σ_l. For NN tilt, $\hat{\mathbf{l}} = \hat{\mathbf{i}}$, while for NNN tilt, $\hat{\mathbf{l}} = \hat{\mathbf{j}}$. Since all the lattice vectors $\mathbf{r_{ij}}$ are in the monolayer plane, we have

$$(r_{\gamma\delta}^{(\pm)})^2 = r_{ij}^2 + z_{\gamma\delta}^2 \pm 2\, z_{\gamma\delta}\, r_{ij,l} \sin(\theta), \tag{A2}$$

where $r_{ij,l}$ is the component of $\mathbf{r_{ij}}$ in the direction of $\hat{\mathbf{l}}$. To simplify notation, we define $s_{\gamma\delta}^{(\pm)} \equiv (r_{\gamma\delta}^{(\pm)})^2$, so that

$$s_{\gamma\delta}^{(\pm)} \equiv s_{\gamma\delta}^{(0)} \pm \Delta s_{\gamma\delta}, \tag{A3}$$

with

$$s_{\gamma\delta}^{(0)} \equiv r_{ij}^2 + z_{\gamma\delta}^2, \quad \Delta s_{\gamma\delta} \equiv 2\, z_{\gamma\delta}\, r_{ij,l} \sin(\theta). \tag{A4}$$

The energy can then be written as

$$E = \sum_{j\neq i} \sum_{\gamma} U_{\gamma\gamma}(r_{ij}^2) + \sum_{j\neq i} \sum_{\gamma<\delta} [U_{\gamma\delta}(s_{\gamma\delta}^{(+)}) + U_{\gamma\delta}(s_{\gamma\delta}^{(-)})]. \tag{A5}$$

A. Expansion in powers of sin(θ)

It is clear from the definition of $s_{\gamma\delta}^{(\pm)}$ and the second term in (A5) that E is an even function of $\sin(\theta)$. As such, for small tilt-angles θ, one can expand the functions $U_{\gamma\delta}(s_{\gamma\delta}^{(\pm)})$ in powers of $\sin(\theta)$ to obtain

$$\begin{aligned} E = &\sum_{j\neq i} \bar{U}(r_{ij}^2) + \left(\sum_{j\neq i} \bar{U}^{(2)}(r_{ij}^2) r_{ij,l}^2 \right) \sin^2(\theta) \\ &+ \left(\sum_{j\neq i} \bar{U}^{(4)}(r_{ij}^2) r_{ij,l}^4 \right) \sin^4(\theta) \\ &+ \left(\sum_{j\neq i} \bar{U}^{(6)}(r_{ij}^2) r_{ij,l}^6 \right) \sin^6(\theta) + \cdots, \end{aligned} \tag{A6}$$

where

$$\begin{aligned} \bar{U}(r_{ij}^2) &\equiv \sum_{\gamma} U_{\gamma\gamma}(r_{ij}^2) + 2 \sum_{\gamma<\delta} U_{\gamma\delta}(s_{\gamma\delta}^{(0)}), \\ \bar{U}^{(2)}(r_{ij}^2) &\equiv \sum_{\gamma<\delta} U_{\gamma\delta}^{(2)}(s_{\gamma\delta}^{(0)})(2z_{\gamma\delta})^2, \\ \bar{U}^{(4)}(r_{ij}^4) &\equiv \frac{2}{4!} \sum_{\gamma<\delta} U_{\gamma\delta}^{(4)}(s_{\gamma\delta}^{(0)})(2z_{\gamma\delta})^4, \\ \bar{U}^{(6)}(r_{ij}^6) &\equiv \frac{2}{6!} \sum_{\gamma<\delta} U_{\gamma\delta}^{(6)}(s_{\gamma\delta}^{(0)})(2z_{\gamma\delta})^6, \end{aligned} \tag{A7}$$

and

$$U_{\gamma\delta}^{(m)}(s_{\gamma\delta}^{(0)}) \equiv \frac{d^m U_{\gamma\delta}(s)}{ds^m}\Big|_{s=s_{\gamma\delta}^{(0)}}. \tag{A8}$$

Let us now examine the coefficients of the $\sin^n(\theta)$ terms in (A6). The coefficient of the $\sin^2(\theta)$ term is

$$\sum_{j\neq i} \bar{U}^{(2)}(r_{ij}^2) r_{ij,l}^2.$$

When tilted in the NN direction $r_{ij,l} = x_{ij}$, and for tilting in the NNN direction $r_{ij,l} = y_{ij}$. With this notation, one can then define the following moments:

$$\langle x^2 \rangle \equiv \sum_{j\neq i} \bar{U}^{(2)}(r_{ij}^2) x_{ij}^2, \quad \langle y^2 \rangle \equiv \sum_{j\neq i} \bar{U}^{(2)}(r_{ij}^2) y_{ij}^2. \tag{A9}$$

By symmetry arguments, we can show that $\langle x^2 \rangle = \langle y^2 \rangle$ on an *undistorted* hexagonal lattice. Consider such a lattice rotated by either $\pm \pi/3$ so that the x and y axes are mapped onto the new axes x' and y' according to the following relations:

$$x = \frac{1}{2} x' \pm \frac{\sqrt{3}}{2} y', \quad y = \frac{1}{2} y' \mp \frac{\sqrt{3}}{2} x'. \tag{A10}$$

Calculating the average of x^2 as defined in (A9), one finds

$$\langle x^2 \rangle = \tfrac{1}{4}\langle x'^2 \rangle + \tfrac{3}{4}\langle y'^2 \rangle + \langle \text{cross terms} \rangle = \tfrac{1}{4}\langle x^2 \rangle + \tfrac{3}{4}\langle y^2 \rangle,$$

and, therefore,

$$\langle x^2 \rangle = \langle y^2 \rangle, \tag{A11}$$

where the cross terms average to zero and the identities $\langle x^2 \rangle = \langle x'^2 \rangle, \langle y^2 \rangle = \langle y'^2 \rangle$ are a result of the fact that the rotated system is physically equivalent to the unrotated system by hexagonal symmetry.

One then concludes that for the undistorted lattice, the coefficient of $\sin^2(\theta)$ in (A6) is the same for tilts toward NN and toward NNN. In a similar fashion, we define the fourth moments as

$$\langle x^4 \rangle \equiv \sum_{j\neq i} \bar{U}^{(4)}(r_{ij}^2) x_{ij}^4, \quad \langle y^4 \rangle \equiv \sum_{j\neq i} \bar{U}^{(4)}(r_{ij}^2) y_{ij}^4. \tag{A12}$$

We then find by analogous symmetry arguments on the undistorted lattice (note that odd orders average to zero)

$$\langle x^4 \rangle = \tfrac{1}{16}\langle x'^4 \rangle + \tfrac{18}{16}\langle x'^2 y'^2 \rangle + \tfrac{9}{16}\langle y'^4 \rangle,$$

and therefore

$$15\langle x^4 \rangle = 18\langle x^2 y^2 \rangle + 9\langle y^4 \rangle. \tag{A13}$$

Similarly,

$$15\langle y^4 \rangle = 18\langle x^2 y^2 \rangle + 9\langle x^4 \rangle. \tag{A14}$$

Comparing (A13) and (A14), we obtain

$$\langle x^4 \rangle = \langle y^4 \rangle.$$

Thus, it is found that to fourth order in the moments there is no difference between NN and NNN states. It is only to sixth order that differences emerge between these two types of tilted configurations, such that one finds

$$\langle x^6 \rangle = \langle y^6 \rangle + \langle y^4 x^2 \rangle - \langle x^4 y^2 \rangle.$$

With these considerations, the energy expansion must then proceed to at least sixth order in $\sin(\theta)$ in order to observe differences between the NN and NNN energies.

B. Expansion in powers of α: Including mixed terms

It has been determined that it is sufficient to expand the energy to sixth order in $\sin(\theta)$ and that the odd-order terms cancel. However, it is required that (A6) also be expanded in terms of the distortion parameter α. Recall that the lattice constants a' and b' of the distorted lattice were defined in terms of α according to (6). On a lattice, the lengths x_{ij}, y_{ij} can be expressed as integer multiples of the lattice constants, hence, it follows that

$$x_{ij}^2=(x_{ij}^{(0)})^2e^{\alpha}, \quad y_{ij}^2=(y_{ij}^{(0)})^2e^{-\alpha}, \tag{A15}$$

where the undistorted lattice distances and components are denoted as $r_{ij}^{(0)}, x_{ij}^{(0)}, y_{ij}^{(0)}$. With these definitions, and also using $r_{ij}^2=x_{ij}^2+y_{ij}^2$, we can perform expansions of the coefficients in (A6) in powers of α. We shall omit the details here (see Ref. 25) and summarize the essential points.

The leading-order term in (A6), independent of tilt angle, has the expansion

$$E_0(\alpha)\equiv\sum_{j\neq i}\bar{U}(r_{ij}^2)=E_0+E_{2\alpha}\alpha^2+E_{3\alpha}\alpha^3+\cdots. \tag{A16}$$

The absence of a linear term in α follows from a symmetry relation analogous to (A11) (although involving a different weighting function in the definition of the moments $\langle x^2\rangle$ and $\langle y^2\rangle$). The coefficient of $\sin^2(\theta)$ in (A6) is

$$\begin{aligned}E_{2\theta}(\alpha)&\equiv\sum_{j\neq i}\bar{U}^{(2)}(r_{ij}^2)r_{ij,l}^2\\&=E_{2\theta}+E_{2\theta,\alpha}\alpha+E_{2\theta,2\alpha}\alpha^2+\cdots.\end{aligned} \tag{A17}$$

The analysis in the previous subsection A applied to the leading undistorted coefficient $E_{2\theta}$, showing this to be independent of tilt direction. However, by similar arguments, it is found that the first-order coefficient, $E_{2\theta,\alpha}$, has the same magnitude but *differs in sign* for tilt toward NN and NNN directions, the consequence of which are discussed in Sec. III A. The term $E_{2\theta,2\alpha}$ generally differs for the two tilt directions, not simply in sign.

The coefficient of $\sin^4(\theta)$ in (A6) has the expansion

$$E_{4\theta}(\alpha)\equiv\sum_{j\neq i}\bar{U}^{(4)}(r_{ij}^2)r_{ij,l}^4=E_{4\theta}+E_{4\theta,\alpha}\alpha+\cdots. \tag{A18}$$

Again, from the analysis in the Appendix, the leading term $E_{4\theta}$ is independent of tilt direction while the term $E_{4\theta,\alpha}$ does show a dependence. Finally, the coefficient of $\sin^6(\theta)$ in (A6),

$$E_{6\theta}(\alpha)=\sum_{j\neq i}\bar{U}^{(6)}(r_{ij}^2)r_{ij,l}^6\approx E_{6\theta}+\mathcal{O}(\alpha), \tag{A19}$$

was shown earlier to depend on tilt direction at lowest order. Collecting the results from (A6) and (A16) to (A19) gives the Landau expansion in (7) in the text.

[1] C. M. Knobler and R. C. Desai, Annu. Rev. Phys. Chem. **43**, 207 (1992).
[2] A. M. Bibo and I. R. Peterson, Adv. Mater. **2**, 309 (1990).
[3] V. M. Kaganer, H. Möhwald, and P. Dutta, Rev. Mod. Phys. **71**, 779 (1999).
[4] G. M. Bommarito, W. J. Foster, P. S. Pershan, and M. L. Schlossman, J. Chem. Phys. **105**, 5265 (1996).
[5] E. Teer, C. M. Knobler, C. Lautz, S. Wurlitzer, J. Kildae, and Th. M. Fischer, J. Chem. Phys. **106**, 1913 (1997).
[6] P. Tippmann-Krayer and H. Möwald, Langmuir **7**, 2303 (1991).
[7] M. C. Shih, M. K. Durbin, A. Malik, P. Zschack, and P. Dutta, J. Chem. Phys. **101**, 9132 (1994).
[8] V. M. Kaganer, I. R. Peterson, R. M. Kenn, M. C. Shih, M. Durbin, and P. Dutta, J. Chem. Phys. **102**, 9412 (1995).
[9] J. P. Bareman and M. L. Klein, J. Phys. Chem. **94**, 5202 (1990).
[10] F. M. Haas, R. Hilfer, and K. Binder, J. Phys. Chem. **100**, 15290 (1996).
[11] F. Schmid, Phys. Rev. E **55**, 5774 (1997).
[12] F. Schmid and H. Lange, J. Chem. Phys. **106**, 3757 (1997).
[13] C. Stadler, H. Lange, and F. Schmid, Phys. Rev. E **59**, 4248 (1999).
[14] C. Stadler and F. Schmid, J. Chem. Phys. **110**, 9697 (1999).
[15] D. R. Swanson, R. J. Hardy, and C. J. Eckhardt, J. Chem. Phys. **105**, 673 (1996).
[16] F. M. Haas, R. Hilfer, and K. Binder, J. Chem. Phys. **102**, 2960 (1995).
[17] V. M. Kaganer and V. L. Indenbom, J. Phys. II **3**, 813 (1993).
[18] V. M. Kaganer, M. A. Osipov, and I. R. Peterson, J. Chem. Phys. **98**, 3512 (1993).
[19] S. M. Balashov and V. A. Krylov, Thin Solid Films **239**, 127 (1993).
[20] C. Lautz, Th. M. Fischer, and J. Kildae, J. Chem. Phys. **106**, 7448 (1997).
[21] T. M. Fischer (private communication, 1999).
[22] M. Scheringer, R. Hilfer, and K. Binder, J. Chem. Phys. **96**, 2269 (1992).
[23] S. B. Opps, B. Yang, C. G. Gray, and D. E. Sullivan (unpublished).
[24] The second-order tilted/untilted transition line estimated by the Approx method in (16)–(19) is very similar to that estimated for a slightly different model by Haas *et al*. (Ref. 16), using a geometric packing argument. The latter argument is based on the *assumption* that $d_o^{\mathrm{LJ}}=r_{tt}^{\min}=2^{1/6}\sigma_{tt}$.
[25] S. B. Opps, Ph. D. thesis, University of Guelph (1999).